



Using ground-based GPS to characterize atmospheric turbulence

T. Nilsson,^{1,2} J. L. Davis,³ and E. M. Hill³

Received 15 July 2009; accepted 30 July 2009; published 29 August 2009.

[1] A new method for measuring and studying atmospheric turbulence is presented. The method uses data from a local network of GPS receivers. The GPS data are processed in a way that assures that the estimated zenith total delays (ZTD) contain the effects of atmospheric turbulence present in the GPS observations. The turbulence is characterized using the spatial structure function for the atmospheric zenith total delay. The structure function is modeled by an expression with unknown parameters which contains information about the turbulence. The unknown parameters are solved by a fit to the observed ZTD variations. We apply the method to GPS data from the Yucca Mountain network, Nevada, USA. The results show that the magnitude of the turbulent variations in that region have a strong seasonal dependence, with much larger variations in summer compared to winter. **Citation:** Nilsson, T., J. L. Davis, and E. M. Hill (2009), Using ground-based GPS to characterize atmospheric turbulence, *Geophys. Res. Lett.*, 36, L16807, doi:10.1029/2009GL040090.

1. Introduction

[2] The amplitude and propagation delay of radio signals propagating through the atmosphere will fluctuate due to atmospheric turbulence. For frequencies below 10 GHz, fluctuation in the propagation delay is the most important effect. These fluctuations can be important error sources in space geodetic techniques such as the Global Positioning System (GPS).

[3] The effects atmospheric turbulence have on radio wave propagation are often modeled using the theory of Kolmogorov turbulence [Tatarskii, 1971; Treuhaft and Lanyi, 1987]. Several experiments to test this model have been performed. For example, the predictions for the variations in propagation delay of signals propagating on paths close to the ground were investigated by Hill *et al.* [1988]. Armstrong and Sramek [1982] studied the correlation between interferometric phase fluctuations observed with different radio telescopes distanced 1–35 km. Using a microwave radiometer, both temporal fluctuations [Jarlemark and Elgered, 1998] and variations as function of direction [Nilsson *et al.*, 2005] can be studied. The results from these investigations can be said to be inconclusive: some investigations found good agreement with the Kolmogorov theory while other investigations indicate

some disagreement between the theory and the experimental results.

[4] The magnitude of the turbulent variations in the propagation delay can be expected to vary both between different locations and as function of time, since it is expected that it is dependent on the water vapor content. However, relatively few studies of, e.g., the seasonal dependence, have been performed. Examples of such studies are Chadwick and Moran [1980], Naudet [1996], and Nilsson *et al.* [2005]. Generally these studies show larger atmospheric variations in summer compared to winter.

[5] A potentially new and useful method for studying and characterizing atmospheric turbulence is to use GPS. With this technique it is in principle feasible to study both temporal and spatial correlations of the atmospheric delay fluctuations. For example, Stoew *et al.* [2001] demonstrated that the spatial correlation of delay fluctuations could be studied using a GPS network with a range of inter-site distances. Here, we use a similar approach to investigate seasonal variation of turbulence parameters for a highly dense, localized GPS network. For this we use GPS data from the Yucca Mountain network in Nevada, USA [Wernicke *et al.*, 2004]. The inter-station distances in this network range over values for which we expect only small variations (10 m) up to distances over which significant variations are expected (100 km).

2. Methods

[6] We characterize the atmospheric turbulence by investigating the fluctuations in the zenith total delay (ZTD), F . The ZTD above location \mathbf{r} is given by:

$$F(\mathbf{r}) = \int_0^\infty [n(\mathbf{r}, z) - 1] dz \quad (1)$$

where z is the vertical coordinate and n the refractive index. The refractive index is a function of temperature, atmospheric pressure and humidity, hence any fluctuations in any of these parameters (e.g., caused by turbulence) will cause fluctuations in n and hence also in the ZTD. Thus it should be possible to get information about the atmospheric turbulence by studying the spatial variations in the ZTD.

[7] To investigate the spatial variations in ZTD between two locations \mathbf{r} and $\mathbf{r} + \mathbf{b}$ we use the (modified) structure function:

$$D(b) = \langle (F(\mathbf{r}) - F(\mathbf{r} + \mathbf{b}) - \langle F(\mathbf{r}) - F(\mathbf{r} + \mathbf{b}) \rangle)^2 \rangle \quad (2)$$

where $b = \|\mathbf{b}\|$ is the baseline length and $\langle \cdot \rangle$ denotes expectation value. We remove the average difference in ZTD since we are only interested in the fluctuations, not any possible average differences between the two locations resulting from the stations being at slightly different alti-

¹Department of Radio and Space Science, Chalmers University of Technology, Göteborg, Sweden.

²Institute of Geodesy and Geophysics, Vienna University of Technology, Vienna, Austria.

³Harvard-Smithsonian Center for Astrophysics, Cambridge, Massachusetts, USA.

tudes. $D(b)$ will be a measure of the magnitude of the atmospheric variations over the distance b . This will of course include both turbulence and other variations, such as the passage of weather fronts and evaporation/condensation of water vapor. Over the distances considered in this work (distances up to a few 100 km) most variations can be expected to be caused by turbulence, while other types of variation get more important over larger distances.

[8] According to Kolmogorov turbulence theory the structure function $D(b)$ should be proportional to $b^{2/3}$ when b is much longer than a few kilometers [Treuhaft and Lanyi, 1987]. In this work we allow for the power-law exponent to be different from $2/3$ since some other investigations indicate other values of α . Furthermore it is likely that there will be (non-atmospheric) noise in our estimated ZTD values. This noise will contribute to the estimated $D(b)$ values. Assuming that the contribution from this noise to $D(b)$ is independent of b , we model the structure function as:

$$D(b) = \sigma_0^2 + C^2 \left(\frac{b}{B_0} \right)^\alpha \quad (3)$$

where σ_0^2 is the variance of the non-atmospheric noise, C^2 is the structure constant, and α is the power-law exponent. In this work we use $B_0 = 100$ km, which is approximately the mean inter-station distance of the network.

[9] The model equation (4) assumes that the ZTD variations will be of the same magnitude independent of the altitudes of the stations. However, in reality we could expect smaller variations at large altitudes since the water vapor content generally decreases with height. Thus we also test using a slightly more advanced model:

$$D(b) = \sigma_0^2 + C^2 e^{-kz} \left(\frac{b}{B_0} \right)^\alpha \quad (4)$$

where z is the mean altitude of the two stations for which $D(b)$ is calculated, and the parameter k represents the inverse scale height of the atmospheric fluctuations.

[10] Both expressions (4) and (5) assume that each $D(b)$ value is calculated using ZTD estimated from two stations located at the same altitude. This is a problem since the Yucca Mountain network contains stations located at altitudes ranging from 100 m to 3 km. To avoid this problem we only use $D(b)$ calculated for pairs of stations with a difference in altitude of ≤ 200 m. In total ~ 200 baselines fulfill that requirement. Another possibility may have been to use a structure constant that takes into account the height differences between the stations, but this was not done in this initial study.

3. Data Analysis

[11] We use the GPS data from the years 2006 and 2007 to estimate the ZTD values used in equation (3). The GPS data were analyzed in a network solution using the GAMIT software [Herring et al., 2006]. In the analysis we used GPS data with a sampling interval of 30 seconds. Ionospheric free linear combination of the two GPS frequencies were used. Satellite orbit parameters were fixed to the “final” values provided by the International GNSS Service (IGS) [Dow et al., 2005]. The station coordinates were estimated, but constrained to values obtained from an analysis of a longer

time-series (in order to have consistency in the ZTD estimates between each day, due to the large correlations between the errors in ZTD and the errors in the coordinates). The coordinates were constrained with an a priori σ of 0.5 mm for the horizontal components and 1 mm for the vertical components. Tidal motions of the stations were modeled according to the IERS conventions [McCarthy and Petit, 2004]. Initial ambiguities were estimated as free parameters and then fixed to integers. The ZTD of each station were estimated in the data processing as piece-wise linear functions in two hour intervals (thus we obtained ZTD estimates with two hour resolution). In the processing we used the mapping functions of Boehm et al. [2006] to relate the ZTDs to the atmospheric delays in the directions of the satellites.

[12] Estimated ZTD values will not correspond exactly to the true delay in the zenith direction, but rather an average of the slant delays between the satellites and the GPS receiver mapped to zenith. In order to have the estimated ZTD correspond as much as possible to the true ZTD, only observations at high elevation angles should be used. By doing that we should also be able to avoid problems with error sources (e.g., multipath) mostly important for low elevation angles. However, the elevation cut-off angle should not be too large since this will increase the uncertainties in the estimated ZTD due to fewer observations and less optimal geometry. We used three different elevation cut-off angles: 30°, 40°, and 50°. Except when otherwise noted, the presented results are a 30° elevation cut-off angle.

[13] We calculated $D(b)$ for each baseline and each month. Each $D(b)$ value was obtained by calculating the difference in ZTD between the two stations of the baseline for each point in time where we had estimated ZTD values. The $D(b)$ value is then obtained by calculating the variance of these differences.

[14] From the obtained $D(b)$ values we estimated the unknown parameters σ_0^2 , C^2 and α (and for equation (4) also k). To do this we used a non-linear least-squares fit. To get as accurate results as possible the observed $D(b)$ should be weighted by their respective uncertainties. These are unknown, however since $D(b)$ is in principle a variance it can be assumed that the uncertainty of the value of $D(b)$ is proportional to $D(b)$. Hence, the error in logarithm of the estimated $D(b)$ can be assumed to be independent of b . Furthermore, the error in $\log D(b)$ will be approximately zero mean if the error in $D(b)$ is zero mean and small compared to $D(b)$. Hence, the non-linear least squares fit is made in logarithmic scale, i.e., for equation (3) we fitted $\log D(b)$ to $\log(\sigma_0^2 + C^2(b/B_0)^\alpha)$ with equal weighting of all $\log D(b)$ values. The non-linear least-squares problem was solved by linearizing the problem around a first guess for the parameter values, solving the linearized problem, then iterating until the solution converged. We also estimated the $1-\sigma$ formal errors by estimating the variance of the observed $\log D(b)$ values as the variance of the residuals after the fit. However, it should be noted that this is likely to underestimate the uncertainties since we assume that the errors of all $D(b)$ estimates are uncorrelated.

4. Results

[15] Figure 1 shows $D(b)$ calculated using the GPS data from the months August 2006 and January 2007, and for the

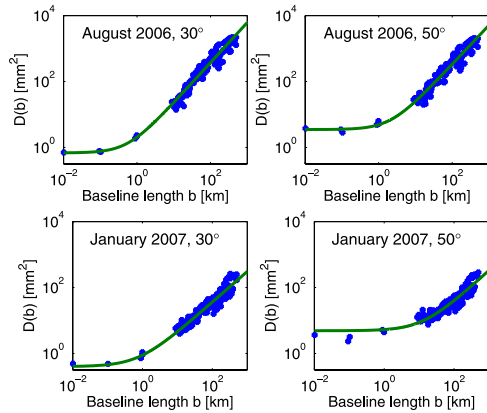


Figure 1. Structure functions $D(b)$ (equation (2)) as a function of baseline length, as estimated by the GPS data. Two one-month periods are shown: (top) August 2006 and (bottom) January 2007. (left) Results using an elevation angle cut-off of 30° and (right) results with an elevation angle cut-off of 50° . Also shown are also the fits to equation (3) (green lines).

cases when using 30° and 50° elevation cut-off angles. As shown, the logarithm of $D(b)$ is rather constant for the smallest baselines, then increasing for longer baselines. The likely reason for this is that the non-atmospheric noise in the estimated ZTDs dominates the calculated $D(b)$ for short baselines, while for longer baselines the actual ZTD variations become larger. The $D(b)$ values for the longer baselines are higher in the August period compared to the January period, indicating that the magnitude of the ZTD fluctuations is larger in summer compared to winter. Furthermore, the $D(b)$ values for the shortest baselines are higher for the case with 50° elevation cut-off angle compared to using 30° , showing that the noise in the ZTD estimates increase when using a larger elevation cut-off angle (as expected). Also shown are the model fits to equation (3). As shown the model fit agrees well with the observed $D(b)$. The differences between the observed and modeled $\log D(b)$ values are relatively independent of the baseline length b , just as we assumed.

[16] Figure 2 shows estimates of C^2 and α as function of time of year. The error bars show the estimated formal $1-\sigma$ uncertainties, representing the uncertainties associated with the GPS observations propagated through the post-analysis method described in the paper. They are not intended to represent the distribution of the “true” atmospheric quantities. The error bars are typically very small, although as noted before they are most likely underestimated. Shown in Figure 2 are the results from the three different solutions, using the three different elevation angle cut-off values.

[17] As seen, the estimates of C^2 vary by almost a factor of 10 between summer and winter. This shows that the turbulent variations are larger in the summer, probably due in part to a higher water vapor content. This is in agreement with the results presented by Nilsson *et al.* [2005], where a seasonal dependence in the magnitude of turbulent variations was also discovered by investigating the variability of the wet part of the atmospheric delay as a function of direction. The delays were measured by a microwave radiometer at Onsala Space Observatory on the Swedish west coast. The observed variations in α are smaller,

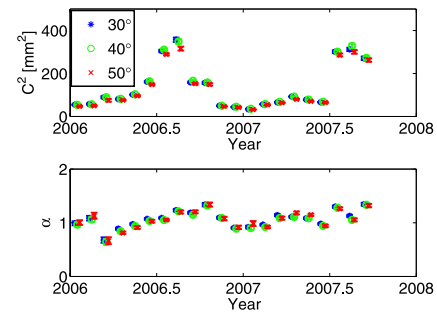


Figure 2. Parameters C^2 and α (equation (3)) estimated from the GPS data for the years 2006 and 2007.

although a small seasonal dependence can be noticed even here. This variation is however similar to the estimated uncertainties in α , and it is not as large and significant as in C^2 . This shows that the structure of the atmospheric turbulence (of which α is a measure) remains relatively constant over the year, even though the amplitude has a significant seasonal variation. The estimated values of σ_0^2 (not shown) are relatively constant over the year and larger when using larger elevation cut-off angle ($\sigma_0^2 \approx 0.6 \text{ mm}^2$ for 30° and $\sigma_0^2 \approx 5 \text{ mm}^2$ for 50°).

[18] The results from the fit to equation (4) can be seen in Figure 3. We do not see any significant difference compared to using equation (3). In general the α values estimated using equation (4) are slightly higher than those estimated using equation (3) (on average ~ 0.05 higher). Much larger values are obtained for C^2 , but this is because C^2 in equation (4) refers to height zero while C^2 in equation (3) refers to an average height of the stations in the network. The seasonal variations in the estimated C^2 and α values are similar to those estimated using equation (3). We can also see that k tends to be smaller in the winter which could mean that the turbulence is decreasing more slowly with height. This might be due to a lower water vapor content, hence the fluctuations in the hydrostatic part of the atmospheric delay will have a larger impact on the results. We even get negative values in one period (although zero is inside the error margins). This result seems at odds with our expectations if we interpret k as the inverse scale height of water vapor (which is positive). It could be due to a local

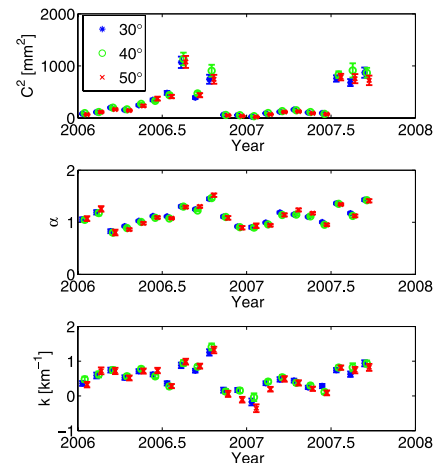


Figure 3. Parameters C^2 , α and k (equation (4)) estimated from the GPS data for the years 2006 and 2007.

phenomena such that turbulence close to the ground predominates at high-altitude locations. However, we can also note that this period has very low C^2 value (21–34 mm² depending on elevation cut-off angle) meaning that the air is not very turbulent during this period, and other error sources might be important (unmodelled station motions, etc.).

[19] The estimated α values are in general larger than the value 2/3 predicted by Kolmogorov turbulence for baselines larger than a few kilometers [Treuhaft and Lanyi, 1987]. The estimated α values are on average 1.05 when using equation (3) and 1.10 when using equation (4). There are of course some baselines much shorter than a few kilometers and for these we would expect $\alpha = 5/3$ [Tatarskii, 1971]. However, since these seem to be dominated by noise, their contribution to the estimated α can be assumed to be very low. One reason for this could be that the theory is incorrect. Several other studies also indicate an exponent slightly higher than 2/3 [e.g., Jarlemark and Elgered, 1998]. It should, however, be noted that the results could have been affected by the spatial and temporal averaging done in the analysis of the GPS data, i.e., using observations of several different directions and describing the ZTD as a piece-wise linear function in two-hour intervals. Thus it will be difficult to see any variations at spatial scales much smaller than the typical distance the air is moving in a two hour period. For typical wind speeds this will correspond to a few tens of km. Thus the fluctuations for the smallest baseline used in this work may be underestimated, hence resulting in an overestimation of α .

[20] In general there is a high agreement between the values estimated using the different elevation cut-off angles. The largest differences are in the estimated values of C^2 , where the average difference between 30° and 50° is ~8%. The estimated α values generally agree within 5% between results from processing with different elevation cut-off angles. The likely reason for the observed differences between different elevation cut-off angles is multipath. The observed differences are, however, generally less than or similar to what could be expected from the uncertainties, hence we do not consider these to be significant.

[21] One potential problem could be unmodelled station motions due to, for example, tectonic deformations [Wernicke et al., 2004]. This is mostly important if there are differences in unmodelled motions between different stations, while a common motion of all stations will not affect our results. We performed a test with slightly looser constraints on the coordinates (10 mm in the vertical direction, 5 mm in horizontal directions). This did not change the results significantly. The largest differences in the estimated C^2 and α values were for the case when using an elevation cut-off angle of 30°. In that case the estimated values changed ~2–3%. This indicates that unmodelled station motions might have had an effect on the results, although the effect is smaller or of a similar size to other error sources.

[22] Another problem could be that the stations are located at different altitudes. To avoid problems related to this we only used baselines with small height differences between the stations. However if the allowed height difference is chosen to be too small the number of useful baselines is very small. We investigated different values for the maximum allowed height difference. We found that the results were not significantly affected when allowing for height differences of up to

500 m, however to have some margins we used 200 m as maximum height difference in this work.

5. Conclusions

[23] We have demonstrated that a dense ground-based GPS network can be used to characterize time-dependent atmospheric fluctuations. Modeling the results as Kolmogorov turbulence, large variation in the parameter C^2 as a function of season is seen, about a factor of 10 between the winter and summer, with the maximum in August.

[24] The estimated values for α are generally larger than the 2/3 predicted by Kolmogorov turbulence theory (the average estimated α for the investigated period is 1.05 when estimated using equation (3)). This indicates that there also exist variations in the ZTDs not described by the Kolmogorov theory. It is likely that some of the error sources, e.g., the fact that we describe the ZTD as a piece-wise linear function, had an impact on this result.

[25] **Acknowledgments.** The research on atmospheric turbulence by Tobias Nilsson was supported by the Swedish National Space Board.

References

- Armstrong, J. W., and R. A. Sramek (1982), Observations of tropospheric phase scintillations at 5 GHz on vertical paths, *Radio Sci.*, 17(6), 1579–1586.
- Boehm, J., A. Niell, P. Tregoning, and H. Schuh (2006), Global Mapping Function (GMF): A new empirical mapping function based on numerical weather model data, *Geophys. Res. Lett.*, 33, L07304, doi:10.1029/2005GL025546.
- Chadwick, R. B., and K. P. Moran (1980), Long-term measurements of C_n^2 in the boundary layer, *Radio Sci.*, 15(2), 355–361, doi:10.1029/RS015i002p00355.
- Dow, J. M., R. E. Neilan, and G. Gendt (2005), The international GPS service: Celebrating the 10th anniversary and looking to the next decade, *Adv. Space Res.*, 36(3), 320–326.
- Herring, T. A., R. W. King, and S. C. McClusky (2006), Introduction to GAMIT/GLOBK, technical report, Dep. of Earth, Atmos., and Planet. Sci., Mass. Inst. of Technol., Cambridge.
- Hill, R. J., R. A. Bohlander, S. F. Clifford, R. W. McMillan, J. T. Priestley, and W. P. Schoenfeld (1988), Turbulence-induced millimeter-wave scintillation compared with micrometeorological measurements, *IEEE Trans. Geosci. Remote Sens.*, 26(3), 330–342.
- Jarlemark, P. O. J., and G. Elgered (1998), Characterizations of temporal variations in atmospheric water vapor, *IEEE Trans. Geosci. Remote Sens.*, 36(1), 319–321.
- McCarthy, D. D., and G. Petit (Eds.) (2004), *IERS Conventions 2003*, *IERS Tech. Note*, vol. 32, Verl. des Bundesamts für Kartographie und Geod., Frankfurt am Main, Germany.
- Naudet, C. J. (1996), Estimation of tropospheric fluctuations using GPS data, *JPL TDA Prog. Rep.*, 42-126, 1–19.
- Nilsson, T., L. Gradinarsky, and G. Elgered (2005), Correlations between slant wet delays measured by microwave radiometry, *IEEE Trans. Geosci. Remote Sens.*, 43(5), 1028–1035, doi:10.1109/TGRS.2004.840659.
- Stoew, B., G. Elgered, and J. M. Johansson (2001), An assessment of estimates of IWV from ground-based GPS data, *Meteorol. Atmos. Phys.*, 77(1–4), 99–107.
- Tatarskii, V. I. (1971), *The Effects of the Turbulent Atmosphere on Wave Propagation*, Isr. Program for Sci. Transl., Jerusalem.
- Treuhaft, R. N., and G. E. Lanyi (1987), The effect of the dynamic wet troposphere on radio interferometric measurements, *Radio Sci.*, 22(2), 251–265, doi:10.1029/RS022i002p00251.
- Wernicke, B., J. L. Davis, R. A. Bennett, J. E. Normandeau, A. M. Friedrich, and N. A. Niemi (2004), Tectonic implications of a dense continuous GPS velocity field at Yucca Mountain, Nevada, *J. Geophys. Res.*, 109, B12404, doi:10.1029/2003JB002832.

J. L. Davis and E. M. Hill, Harvard-Smithsonian Center for Astrophysics, MS 42, 60 Garden Street, Cambridge, MA 02138, USA. (jdavis@cfa.harvard.edu; ehill@cfa.harvard.edu)

T. Nilsson, Department of Radio and Space Science, Chalmers University of Technology, SE-412 96 Göteborg, Sweden. (tobias.nilsson@chalmers.se)